Image effects of cylindrical pipes on continuous beams

Christopher K. Allen and Martin Reiser
Institute for Plasma Research, University of Maryland, College Park, Maryland 20742
(Received 13 October 1995; revised manuscript received 22 March 1996)

We analyze the image effects of a cylindrical pipe on continuous beams with elliptical symmetry. Differential equations involving the second-order spatial moments of a particle distribution are given. From the moment equations, a set of Kapchinskij-Vladimirskij-type equations is developed, which include the image effects of a cylindrical beam pipe. These equations are used to analyze the image effects for focusing, drift, defocusing, drift channels, sheet beams, and a magnetic quadrupole matching section. [S1063-651X(96)08209-8]

PACS number(s): 41.85.−p

I. INTRODUCTION

In most accelerator applications a particle beam must propagate through a conducting beam pipe. If the beam dimensions are comparable to the pipe dimensions then the image forces from the pipe will affect the beam dynamics. Usually these are unwanted effects, so by studying such phenomena we hope to develop techniques to reduce their influence. In previous works we have analyzed image effects for axisymmetric bunched beams in cylindrical pipes [1,2]. In this paper we continue the analysis for continuous beams having elliptical symmetry. The primary application of these results would be the analysis of magnetic quadrupole transport systems.

Here we consider continuous beams centered on the z axis, the axis of propagation, having elliptical symmetry. By elliptical symmetry, we mean that the beam is symmetric across the planes $x=0$ and $y=0$. Elliptical symmetry also implies that the (transverse) charge density of the beam must be constant along concentric ellipses. We assume the beam pipe to be cylindrical with radius b. We also assume the pipe to be perfectly conducting and, for necessity in constructing the Green's function, we hold it at ground potential (this does not affect the analysis). Figure 1 depicts the example situation of a uniform elliptical distribution in a cylindrical pipe. A transverse cross section of the beam and beam pipe is shown lying in the xy plane. The beam is centered on the z axis (not shown) corresponding to the point $(x,y)=(0,0)$. The beam has x envelope a_x, and y envelope a_y. Of course, for more general distributions a_x and a_y will no longer be the x and y envelopes of the beam, but will be the major and minor semiaxes of ellipses along which the charge density is constant.

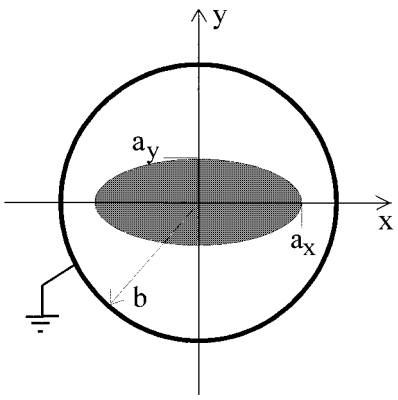

FIG. 1. Example geometry of ellipsoidally symmetric uniform beam in a cylindrical pipe.

A. The equivalent beam concept

Our work is essentially an extension to the results of Sacherer [3]. He derived a set of coupled, ordinary differential equations that describe the evolution of the rms beam envelope for all continuous beams having elliptical symmetry. These equations have the same functional form as the Kapchinskij-Vladimirskij [4] coupled-envelope equations (KV equations). Indeed, for the uniform distribution these equations are the KV equations exactly. Sacherer's result led to the idea of the equivalent KV beam.

Sacherer's formalism allows us to model any continuous beam having elliptical symmetry with an equivalent KV beam. This equivalent beam is a uniform-density, continuous beam having elliptical cross section and having the same second moments as the actual beam under study. The second spatial moments are called the rms envelopes of the beam. The KV equivalent beam has beam envelopes twice that of the actual beam's rms beam envelopes. Also, the emittances of the equivalent beam, called the effective emittances, are four times the rms emittances of the actual beam. Thus, the KV coupled-envelope equations may be used to model any continuous beam with elliptical symmetry if the rms beam envelopes and effective emittance values are used in the equation.

The main achievement of our work is the addition of terms to the KV equations that describe the dominant effects of a cylindrical beam pipe. More specifically, we extend Sacherer's equations to include the first-order image effects due to the beam pipe. We then translate these equations to that of the equivalent KV beam. The result is the original KV equations with a term added (to each equation), which accounts for images.

B. Limitations and assumptions

The major shortcoming of this work is the assumption that the rms emittances are constant or known *a priori*. The

forehand knowledge of the rms emittances through the beam channel is usually an unrealistic expectation. Since rms emittance growth may occur with nonlinear forces (and the image forces are typically nonlinear), the assumption of constant emittances leaves us with a potentially inconsistent analysis. Thus, it would seem that the best utilization of our work would be to determine under what conditions image forces play a significant role in the beam dynamics, rather than the precise prediction of beam behavior under the influence of image forces.

In this paper we neglect longitudinal effects. That is we assume that the continuous beam expands and contracts gradually enough to ignore the longitudinal self-fields. Also, this implies that the focusing system is ideal in that no axial forces are produced. With these assumptions we may treat each cross section of the beam independently. The transverse motion is decoupled from the longitudinal motion and only the transverse self-forces and focusing forces affect the beam at each cross section. Thus, for each axial location z we may describe the beam by a distribution function of the transverse phase-space variables x, x', y, and y'.

II. THE ENVELOPE EQUATIONS WITH IMAGES

Let $\langle\ \rangle$ denote the moment operator with respect to the particle beam distribution. It is possible to derive a set of coupled differential equations for the second spatial moments $\langle x^2\rangle$ and $\langle y^2\rangle$ of the particle beam distribution [3],

$$\begin{aligned}\langle x^2\rangle'' - \frac{[\langle x^2\rangle']^2}{2\langle x^2\rangle} + \frac{2k_x(z)}{\gamma m\nu^2}\langle x^2\rangle - \frac{2q}{\gamma m\nu^2}\langle xE_x\rangle - \frac{2\tilde{\epsilon}_x^2}{\langle x^2\rangle} = 0,\\ \langle y^2\rangle'' - \frac{[\langle y^2\rangle']^2}{2\langle y^2\rangle} + \frac{2k_y(z)}{\gamma m\nu^2}\langle y^2\rangle - \frac{2q}{\gamma m\nu^2}\langle yE_y\rangle - \frac{2\tilde{\epsilon}_y^2}{\langle y^2\rangle} = 0,\end{aligned} \tag{1}$$

where the prime indicates differentiation with respect to z, q is the particle charge, m is the particle mass, ν is the beam's axial velocity, $-k_x(z)x$ is the focusing force in the x direction, and E_x is the beam's self-field in the x direction. We have similar definitions for $-k_y(z)y$ and E_y in the y direction. The symbols $\tilde{\epsilon}_x$ and $\tilde{\epsilon}_y$ represent the rms emittances in the x and y planes, respectively. For systems where all forces are linear, it is known that the rms emittances are invariant [5]. If there exist nonlinear forces (say in E_x) we simply assume that either $\tilde{\epsilon}_x$ is constant or its variation is known *a priori*.

The only unknowns in Eqs. (1) are $\langle xE_x\rangle$ and $\langle yE_y\rangle$. Sacherer computed these quantities for the free-space situation. He found the surprisingly simple result

$$\langle xE_x\rangle = \frac{qN}{4\pi\epsilon_0}\frac{a_x}{a_x+a_y} = \frac{qN}{4\pi\epsilon_0}\frac{\langle x^2\rangle^{1/2}}{\langle x^2\rangle^{1/2}+\langle y^2\rangle^{1/2}}, \tag{2}$$

with an analogous result for $\langle yE_y\rangle$. Note that the above expression is independent of the distribution; this condition leads to the notion of KV equivalent beams. Also, the above expression provides coupling between the two equations in (1). Substituting this expression for $\langle xE_x\rangle$ in Eqs. (1) leads to Sacherer's equations for the rms beam envelopes $\langle x^2\rangle^{1/2}$ and $\langle y^2\rangle^{1/2}$. However, we wish to include the effects of images in this model. We compute the fields including images using Green's function in polar coordinates. By expanding Green's function in a trigonometric series, we can identify the terms corresponding to the induced (image) charges on the beam pipe. Taking the moments of these fields we get [6]

$$\begin{aligned}\langle xE_x\rangle = \frac{qN}{4\pi\epsilon_0}\Bigg[\frac{\langle x^2\rangle^{1/2}}{\langle x^2\rangle^{1/2}+\langle y^2\rangle^{1/2}} + 2\frac{\langle x^2\rangle}{b^4}(\langle x^2\rangle - \langle y^2\rangle)\\ + O\left(\frac{\langle x^4\rangle^2}{b^8}, \frac{\langle x^4\rangle\langle y^4\rangle}{b^8}, \frac{\langle y^4\rangle^2}{b^8}\right)\Bigg],\end{aligned} \tag{3}$$

where $O(\ )$ indicates the standard order notation. The first term in the above equation represents the free-space contribution to $\langle xE_x\rangle$, while the second term represents the contribution due to the induced charges from the distribution's quadrupole moment. The last term is intended to indicate that the image forces due to the higher-order moments of the charge distribution (octupole moments and up) scale as $\langle x^4\rangle^2/b^8$, etc.

By substituting Eq. (3) into Eqs. (1) we have moment equations that include the first-order image effects. However, it is the KV equivalent beam that is of interest. Defining the envelopes of the KV equivalent beam in the x and y planes by $X(z)$ and $Y(z)$, respectively, we know that

$$X = 2\langle x^2\rangle^{1/2}, \quad Y = 2\langle y^2\rangle^{1/2} \tag{4}$$

for this beam. Collecting these results and substituting them into Eqs. (1) yields the following set of equations for the equivalent KV beam:

$$\begin{aligned}X'' + \kappa_x(z)X - \frac{2K}{X+Y} - \frac{\epsilon_x^2}{X^3} - \frac{K}{4b^4}(X^3 - XY^2) = 0,\\ Y'' + \kappa_y(z)Y - \frac{2K}{X+Y} - \frac{\epsilon_y^2}{Y^3} - \frac{K}{4b^4}(Y^3 - YX^2) = 0,\end{aligned} \tag{5}$$

where $K = qI/(2\pi\epsilon_0\gamma m\nu^3)$ is the generalized beam perverance [7] (I being the beam current), and $\kappa_x(z) = k_x(z)/(\gamma m\nu^2)$ and $\kappa_y(z) = k_y(z)/(\gamma m\nu^2)$ are the focusing functions in the x and y planes, respectively. The quantities ϵ_x and ϵ_y are the effective emittances of the beam given by $4\tilde{\epsilon}_x$ and $4\tilde{\epsilon}_y$, respectively. These equations are recognized as the standard KV coupled-envelope equations with the addition of a term (for each equation) accounting for the dominant image effects. Since the beam is centered and has elliptical symmetry, $\langle x^3\rangle$ is zero and the next image term will be an octupole term.

III. EXAMPLES AND ANALYSIS

We may use Eqs. (5) to explore the effects of the beam pipe on the beam dynamics. In this section we present three example situations to determine the significance of image effects in typical applications. The first example is a periodic transport channel made of (magnetic) quadrupole lenses. We treat this example completely analytically by comparing the relative strengths of the competing terms in Eqs. (5). The second example is the approximate analysis of a sheet beam in a cylindrical pipe. The third example is a matching section for a quadrupole transport channel used in the University of Maryland's Electron Ring Experiment [8,9]. In this example

we numerically integrate Eqs. (5) to analyze the effects of images.

A. Periodic transport channel

Consider a periodic transport channel made up of magnetic quadrupoles in a FODO arrangement (focusing, drift, defocusing, drift). Assume that we have a matched beam with equal x and y emittances. In addition assume that the FODO channel is symmetric, that is, it has equal focusing and defocusing strengths in each plane. In such a periodic channel, the beam envelopes X and Y will oscillate 180° out of phase with each other. We denote the minimum and maximum beam envelope excursions for these oscillations (for both planes) as $X_{\min}$ and $X_{\max}$, respectively. Therefore, at some axial location X will be at a maximum (with value $X_{\max}$) and Y will be at a minimum (with value $X_{\min}$). This position will be the location of maximum image effects. It will be our goal to find the channel parameters that will keep the image forces below a given tolerance factor T.

Since we are interested in space-charge dominated particle beams, we start by analyzing the ratio of the image term to the space-charge term [in such a beam $2K/(X+Y)$ will be the dominant self-term]. To maintain our tolerance, this ratio must be less than the prescribed value T. At the axial location where image forces are maximum this ratio is

$$\frac{R}{4b^4}\, X_{\max}(X_{\max}^2 - X_{\min}^2), \tag{6}$$

where R denotes the average radius of the beam; for the periodic channel we have $R=(X_{\max}+X_{\min})/2$. We may parametrize the maximum and minimum beam excursions by introducing the ripple parameter Δ. This parameter is defined as follows:

$$X_{\max}=(1+\Delta)R, \quad X_{\min}=(1-\Delta)R. \tag{7}$$

Inserting these values into Eq. (6) yields

$$\frac{R^4}{b^4}\,(\Delta+\Delta^2). \tag{8}$$

Thus, to keep the image effects less than a factor T of the overall beam dynamics we must have

$$\frac{R}{b} < \left[\frac{T}{\Delta+\Delta^2}\right]^{1/4}. \tag{9}$$

To get a flavor for this requirement we apply this formula to some typical numbers. If we pick a large but reasonable value for the ripple factor, say 0.3, we find that to maintain a tolerance factor of $T=0.10$ (10% tolerance) the ratio R/b must be less than 0.7, which means that $X_{\max}$ is less than $0.9b$. For $T=0.05$ (5% tolerance) we find that R should be less than $0.6b$ and $X_{\max}$ less than $0.8b$. Thus, these effects should be minimal in most situations. Only when the beam fills a substantial portion of the beam pipe and is sufficiently eccentric (round beams do not experience image effects) will images play a significant role.

For an emittance dominated beam we form the ratio between the image term and the emittance term. At our point of maximum X excursion we find this ratio to be

$$\frac{K}{\epsilon_x^2}\,\frac{R^6}{b^4}\,(1+\Delta)^4\Delta. \tag{10}$$

We can simplify the analysis by realizing for the emittance-dominated beam the emittance term must be much greater than the perveance term. This requirement yields the inequality

$$\frac{\epsilon_x^2}{K} \gg R^2(1+\Delta)^3. \tag{11}$$

To satisfy the above, let us say that $\epsilon_x^2/K = GR^2(1+\Delta)^3$, where G is a large number. Then for a tolerance factor T we find from Eq. (10) that

$$\frac{R}{b} < \left[\frac{GT}{\Delta+\Delta^2}\right]^{1/4}. \tag{12}$$

Comparing this equation with Eq. (9) we see that the image forces for an emittance-dominated beam can potentially be more significant because of the factor $G^{1/4}$.

B. Sheet beam

We may use the results of Sec. II to approximate the image effects on a sheet beam in a cylindrical pipe. For such a beam we assume that the beam dimensions are much larger in one plane than in the other. The result is a beam that is fairly flat, or a sheet. These types of beams are used in free-electron lasers, for instance. We only consider the space-charge dominated regime. Again, it will be our goal to determine the design parameters which maintain the image effects below a given tolerance T.

We assume that the x plane has the larger beam dimension. Therefore, the image effects will be at a maximum when X has a maximum, call this $X_{\max}$, and Y has a minimum, call this $Y_{\min}$. Let ν denote the ratio of $X_{\max}$ to $Y_{\min}$, that is,

$$\nu \equiv \frac{X_{\max}}{Y_{\min}}. \tag{13}$$

Typically ν will have values of five or larger for sheet beams. We mention that the y plane emittance will be about ν times the x plane emittance due to beam compression. However, since we are only interested in the space-charge dominated situation we do not consider this effect. As before, we form the ratio of the image term to the space-charge term in Eqs. (5) to analyze the effects of images. Letting T denote the tolerance factor for the image effects, we have

$$\frac{1}{8b^4}\, X_{\max}(X_{\max}^2 - Y_{\min}^2)(X_{\max}+Y_{\min}) < T \tag{14}$$

for the x plane and

$$\left|\frac{1}{8b^4}\, Y_{\min}(Y_{\min}^2 - X_{\max}^2)(Y_{\min}+X_{\max})\right| < T \tag{15}$$

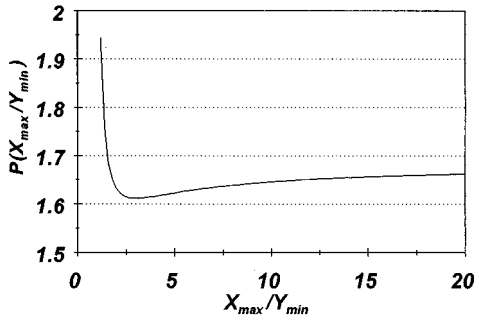

FIG. 2. Image effect tolerance function for a sheet beam.

for the y plane. Note that in this situation the image forces are defocusing in the x plane and focusing in the y plane [thus, the absolute value is necessary in Eq. (15)]. Solving Eq. (13) for $X_{\min}$ and then substituting into the above two equations yields

$$\frac{X_{\max}}{b}<\left[\frac{8\nu^3}{\nu^3+\nu^2-\nu-1}\right]^{1/4}T^{1/4} \tag{16}$$

for the x plane and

$$\frac{X_{\max}}{b}<\left[\frac{8\nu^4}{\nu^3+\nu^2-\nu-1}\right]^{1/4}T^{1/4} \tag{17}$$

for the y plane. Since ν is always greater than 1, the y plane's requirement is automatically satisfied whenever the x plane's tolerance is met. Thus, we need only consider Eq. (16).

We may rewrite Eq. (16) as

$$\frac{X_{\max}}{b}<P(\nu)T^{1/4}, \tag{18}$$

where $P(\nu)$ is the function defined by

$$P(\nu)\equiv\left[\frac{8\nu^3}{\nu^3+\nu^2-\nu-1}\right]^{1/4}. \tag{19}$$

The function $P(\nu)$ is plotted in Fig. 2. It blows up at the point $\nu=1$ (since there are no image effects for a round beam) then asymptotically approaches $8^{1/4}$ as ν approaches infinity. Note, however, that at $\nu=3$ there is an absolute minimum of $P(\nu)$ in the interval $[1,\infty)$. This suggests a resonance condition in the beam pipe. Therefore, to maintain the safest possible margin, the ratio $X_{\max}$ to b should always be kept below the value $P(3)T^{1/4}=(27/4)^{1/4}T^{1/4}\approx 1.61T^{1/4}$. For the tolerances of $T=0.05$ (5%) and $T=0.10$ (10%) this would require $X_{\max}<0.76b$ and $X_{\max}<0.91b$, respectively.

To get an appreciation for the full condition, consider the case where $\nu=5$ and we want a 10% tolerance ($T=0.1$). We find that $X_{\max}$ must be less than $0.92b$. This condition should be fairly easy to meet in order to ignore image effects. For the more demanding case of $\nu=10$ and a 5% tolerance ($T=0.05$) we must have $X_{\max}<0.78b$ to avoid significant effects from images. Obviously in this situation the designer must be much more conscious of the role of images. Finally, we note that as ν becomes large, say greater than 10, the tolerance condition approaches $X_{\max}<8^{1/4}T^{1/4}b$ and is essentially independent of the ratio ν. To compare this situation with the safest tolerance margin (evaluating P at $\nu=3$) consider the tolerances of $T=0.05$ and 0.10. This requires $X_{\max}<0.80b$ and $X_{\max}<0.95b$, respectively.

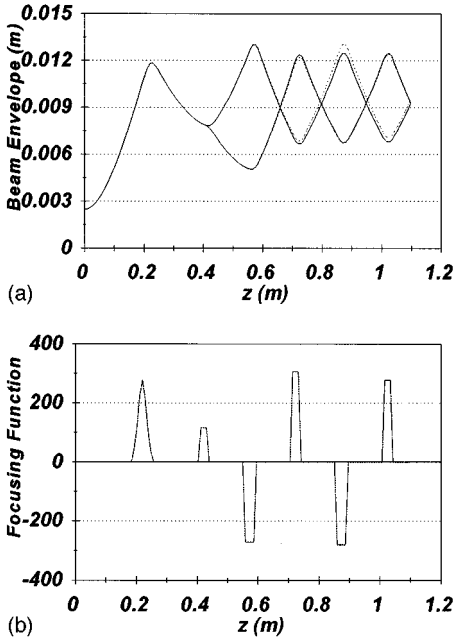

FIG. 3. Image effects for a magnetic quadrupole matching system. The solid lines in (a) represent the x and y envelopes of the free-space solution while the dotted lines represent the solution in the presents of a pipe of radius 1.5 cm.

C. Quadrupole matching section

In the University of Maryland's Electron Ring Experiment a matching section of five lenses matches an electron beam from the cathode source to a transport channel composed of magnetic quadrupole lenses. The matching section is composed of one (initial) solenoid lens followed by four magnetic quadrupole lenses. The quadrupole lenses are arranged so that they have the same axial locations as the lenses in the transport channel, but their focusing strengths remain adjustable. Figure 3(a) shows the simulation results obtained with a fourth-order Runge-Kutta integration of Eqs. (5). In the figure, both the X and Y envelopes of the beam are shown with and without image effects from a beam pipe with radius $b=1.5$ cm. The solid lines represent the free-space solution while the dashed lines show the solution with image effects from the pipe. Figure 3(b) shows the focusing function $\kappa_x(z)$ for the matching section. Since the first lens is a solenoid, it has focusing in both planes; the X and Y envelopes do not separate until the beam passes through the second lens.

One can see that the image effects do not play a large role in the beam dynamics. However, one can also see that the beam will no longer be matched to the transport channel, so it is not an insignificant effect here. Matching sections, overall, will probably be more susceptible to image effects since the beam envelopes tend to make larger excursions through them. In this example we did not see an appreciable effect until the beam pipe radius was decreased to 1.5 cm. Notice

that the images affect the beam most around the axial location $z = 0.6$ m, where the difference in the X and Y envelopes is at a maximum and the beam's Y envelope fills 87% of the pipe. At this point the Y envelope experiences a slight defocusing due to the pipe and subsequently remains larger than its free-space trajectory.

IV. CONCLUSION

We have found that under certain circumstances image effects play a significant role in the dynamics of continuous beams having elliptical symmetry. When the beam is sufficiently eccentric and fills out a substantial portion of the beam pipe, the image forces notably affect the beam dynamics. In practice, these situations will most likely occur in matching sections where the beam experiences large eccentricities and large excursions through the beam pipe. In circumstances where the beam envelope excursions are less extreme, that is, they do not deviate much from the average radius, we expect the image forces considered here to be insignificant. In such situations perhaps a more important effect from images would be due an off-centered beam. Here the image forces would draw the entire beam farther off its center position. This effect is widely known and is covered in Ref. [7], Chap. 4.

As mentioned previously, this approach is not self-consistent. Unless we are fortunate enough to know the rms emittances along the channel, we must assume that they are constant, which is artificial. Since the image effects are nonlinear, the rms emittances will typically increase through the channel, violating the assumption of constant emittances. However, for space-charge dominated situations the increased emittance is a minor effect. Thus, our model will still yield meaningful results. More important, we have a way not only to simulate the beam dynamics with images but also to quantify analytically when these effects will play a significant role. It would seem that the best design strategy is to avoid such effects. The work presented in this paper will give the designer an easy way to check that his or her design will reduce any unwanted influences from image forces.

ACKNOWLEDGMENTS

The authors want to thank Richard Cooper for many useful suggestions and corrections in preparing the manuscript. This work was supported by the U.S. DOE.

[1] C. K. Allen, N. Brown, and M. Reiser, Particle Accel. **45**, 149 (1994).

[2] C. K. Allen and M. Reiser, Particle Accel. **48**, 193 (1995).

[3] F. R. Sacherer, IEEE Trans. Nucl. Sci. **18**, 1105 (1971).

[4] I. M. Kapchinskij and V. V. Vladimirskij, in *Proceedings of the International Conference on High-Energy Accelerators and Instrumentation* (CERN, Geneva, 1959), pp. 274–288.

[5] D. D. Holm, W. P. Lysenko, and J. C. Scovel, Math. Phys. **31**, 1610 (1990).

[6] For the details of this calculation see C. K. Allen and M. Reiser, Institute for Plasma Research, University of Maryland, CPBL Technical Report No. 96-001, 1996 (unpublished).

[7] For a description of this parameter see M. Reiser, *Theory and Design of Charged Particle Beams* (Wiley, New York, 1994), pp. 197 and 257.

[8] M. Reiser, S. Bernal, A. Dragt, M. Venturini, J. G. Wang, H. Onishi, and T. F. Godlove, Fus. Eng. Design (to be published).

[9] S. Bernal, A. Dragt, M. Reiser, M. Venturini, and J. G. Wang, Fus. Eng. Design (to be published).